Available online at www.sciencedirect.com
SCIENCE DIRECT®
Carbon 44 (2006) 99–106
CARBON
www.elsevier.com/locate/carbon

Electrochemical and chemical redox doping of fullerene (C_{60}) peapods ☆

Ladislav Kavan [a,*], Martin Kalbáč [a,b], Markéta Zukalová [a], Lothar Dunsch [b]

[a] J. Heyrovský Institute of Physical Chemistry, Academy of Sciences of the Czech Republic, Dolejškova 3, CZ-182 23 Prague 8, Czech Republic
[b] Leibniz Institute of Solid State and Materials Research, Helmholtzstr. 20, D-01069 Dresden, Germany

Received 24 April 2005; accepted 2 July 2005
Available online 22 August 2005

Abstract

Different types of redox doping of C_{60}@SWCNT were monitored by Raman spectroscopy. Chemical doping was carried out by gaseous potassium, liquid potassium amalgam and gaseous fluorine diluted with argon. Electrochemical doping was investigated by in situ Raman spectroelectrochemistry in $LiClO_4$ + acetonitrile solution and in 1-butyl-3-methylimidazolium tetrafluoroborate (ionic liquid). The peapods exhibit characteristic and complex feedback to chemical as well as to electrochemical doping. In contrast to chemical p-doping by F_2, the Raman scattering of intratubular fullerene is selectively enhanced during electrochemical p-doping. Similar selective enhancement is traced at chemical n-doping with gaseous potassium. Doping by gaseous potassium causes deep reduction of intratubular C_{60} to C_{60}^{6-}, which is not fully re-oxidizable upon contact to air. On the other hand, doping with liquid potassium amalgam causes reduction of intratubular C_{60} to C_{60}^{4-} or C_{60}^{5-}, and complete re-oxidation to neutral fullerene occurs spontaneously upon contact to air. In general, the doping chemistry of peapods is significantly dependent on the applied redox potential, charge-compensating counterions and on the actual doping technique used. A critical review of the current data is provided.

Keywords: Carbon nanotubes; Fullerene; Raman spectroscopy; Electrochemical properties

1. Introduction

In 1998 Smith et al. [1] discovered that fullerene peapods, C_{60}@SWCNT (SWCNT = single wall carbon nanotube) occur naturally in SWCNTs from laser-vaporized graphite, albeit in low concentrations, ca. 4–5.4% (expressed as the filled fraction of total tube length) [2]. Considerable improvement of the filling was achieved by deliberately inserting fullerene into opened SWCNTs from the gas phase at elevated temperatures [3–5]. The optimum diameter of SWCNT for encapsulation of C_{60} is between 1.3 and 1.4 nm, which sets the "graphite-like spacing" (≈0.3 nm) between the C_{60} cage and the tube wall. The C_{60} molecules in peapods represent a 1D-crystal with a lattice constant of (0.95–0.977) nm, which is smaller than the lattice constant in ordinary cubic C_{60} crystal (1.00 nm) [6]. The optimum-sized tubes are produced in high yield via catalytic laser ablation of graphite. By using this synthetic protocol, Kataura et al. [6] obtained peapod material with 85% filling ratio, as determined by X-ray diffraction. Other analytical methods for determination of peapods filling comprise Raman spectroscopy [7] and electron-energy-loss spectroscopy [8], but a simple extraction of C_{60} from acid-mineralized peapod is also a convenient analytical tool [2].

☆ Presented at the 83rd Bunsen Discussion Meeting, Dresden, October 24–27, 2004.

* Corresponding author. Tel.: +420 2 6605 3975; fax: +420 2 8658 2307.
E-mail addresses: kavan@jh-inst.cas.cz (L. Kavan), l.dunsch@ifwdresden.de (L. Dunsch).

0008-6223/$ - see front matter © 2005 Elsevier Ltd. All rights reserved.
doi:10.1016/j.carbon.2005.07.002

Raman spectra of peapods roughly exhibit the superposition of weak lines of C_{60} with strong lines of the SWCNT [6,7,9–11]. There is no significant overlap of the Raman features of C_{60} ($2A_g + 8H_g$) and SWCNT in peapods, except for the $H_g(8)$ band, which coincides with the G-mode of SWCNT. For the excitations around 2.5 eV, the Raman features of C_{60} are resonance enhanced via the first allowed transitions in C_{60} ($h_u \rightarrow t_{1g}, t_{1u}$). However, the matching of Raman spectra of peapods and those of the individual parent components is not perfect. The most explicit discrepancy is a red-shift and splitting of the pentagonal pinch $A_g(2)$ mode providing a high-frequency satellite line $A_g(2)'$. This unexpected splitting of a totally symmetric, non-degenerate mode was interpreted as a result of its coupling to the C_{60} translation [12].

Redox doping of peapods provides useful information about their electronic structure. In general, n-/p-doping increases the concentration of electrons and holes, respectively, and thus modifies the population of electronic states near the Fermi level of SWCNT (pod). In the simplest model, p-doping just extracts electrons from the valence band, and n-doping just pumps electrons into the conduction band, which causes the corresponding shifts of the Fermi level of SWCNT (pod). When the p-/n-doping progresses, the optical transitions between van Hove singularities (vHs) are erased. This causes a bleaching of the tube-related Raman scattering, since it is strongly resonance enhanced via the optical transitions between particular vHs.

This model assumes all doping-driven changes of electron density to occur on the SWCNT (pod), i.e. the C_{60} (pea) remains neutral. This approximation seems to be applicable for mild p-doping with $FeCl_3$ vapor [13]. Pichler et al. [13] estimated that, even at the saturation-doping with $FeCl_3$, the Fermi level is shifted by ca. 0.9 eV into the valence band. This is equivalent to a charge transfer of 0.05 h^+/C-atom [13]. For typical pods (such as metallic (10, 10) and semiconducting (11, 9) SWCNTs) this would cause a quenching of the first optical transition between vHs in metallic tubes (E_{11}^{M}) and first two transitions in semiconducting tubes (E_{11}^{S}, E_{22}^{S}), but the third transition, E_{33}^{S} is unaffected. Consequently, the Raman scattering is intact, if it is enhanced through the E_{33}^{S} transition (for blue–green lasers), but is bleached for the red lasers. Qualitatively similar effects are assumed during mild n-doping with potassium vapor [11,13]. Since, however, potassium is a very strong reductant, progressive doping with K-vapor may even quench the third transition, E_{33}^{S}. Heavy K-doping causes the reduction of C_{60} peas up to C_{60}^{6-} [11,13,14] and their transformation into metallic polymer $(C_{60}^{6-})_n$ [11,13]. EELS further evidences the existence of free-charge-carrier plasmons at ca. 1.3–1.45 eV in K-doped peapods [15].

Chemical redox doping of nanocarbons in general, and peapods in particular, has two principal limitations. First, the palette of chemical oxidants/reductants (electron acceptors/donors, A/D) is restricted only to a small number of molecules, which are able of acting as net e^-/h^+ donors, without causing irreversible chemical modifications of the nanocarbon surface:

$$A + C_{60}@SWCNT \rightarrow A^- + [C_{60}@SWCNT]^+ \quad (1a)$$

$$D + C_{60}@SWCNT \rightarrow D^+ + [C_{60}@SWCNT]^- \quad (1b)$$

(In the case of peapods, only K and $FeCl_3$ were used up to now [11,13,14]). Second, the amount of extra charge e^-/h^+ transferred to nanocarbons is poorly controlled during the contact of gaseous reactant (A/D) with the solid sample. Chemical doping can, in principle, be tuned by varying the time of interaction with gaseous reactant (A/D) [13], but the actual doping level (concentration of the counterion (A^-/D^+)) and its homogeneity in the bulk substrate is out of control.

These problems are elegantly minimized, if the redox doping is carried out electrochemically. In this case, the e^-/h^+ charge transfer occurs via an electrical contact of the nanocarbons to an inert electrode (Pt, Au, Hg, ITO) and the A^-/D^+ species are just electrolyte counterions. The doping is, actually, like a double-layer charging, which is fast and homogeneous over the whole electrochemical interface, and the transferred charge is easily quantified by the electrode capacitance. Second, the palette of counterions, A^-/D^+ is quite rich, from solvated ions occurring in classical electrolyte solutions [9,10,14] to "naked" ions in ionic liquids [16]. (For chemical doping, the counterions, A^- or D^+ cannot be varied that simply, as they are generated by the reaction itself, cf. Eqs. (1a) and (1b)). The benefit of broad selection of counterions is highlighted in studies aimed at diameter- and counterion-sensitive doping [17].

The charging of peapods is most easily monitored by cyclic voltammetry [10,16]. There is no evidence for Faradaic processes of intratubular C_{60}, even at potentials, when the triply charged fulleride anions would be formed from the free C_{60} molecule [9,10,16]. Instead, the voltammetric current, I was found to be simply proportional to the scan rate, v [10,16] as it is expected for purely capacitive process:

$$I = \frac{dQ}{dt} = mC\frac{dU}{dt} = mCv \quad (2)$$

where m is the mass of active electrode material, Q is the voltammetric charge, C is specific capacitance (in F/g) and dU/dt is the scan rate, v. The number of extra charges (electrons/holes), Δf introduced by charging between the open circuit potential, U_{OCP} and certain doping potential, U, is

$$\Delta f = \frac{M_C}{F}\int_{U_{OCP}}^{U} C\,dU \quad (3)$$

where M_C is atomic weight of carbon, and F is Faraday constant. Eq. (3) can be simplified if C is potential-independent in a certain region of $\Delta U = (U - U_{OCP})$:

$$\Delta f = \frac{M_C C \Delta U}{F} \quad (4)$$

For the typical value of $C \cong 40$ F/g (see below), and $\Delta U = 1$ V, Eq. (4) yields $\Delta f \cong 0.005$ h^+/C-atom. This would provide comparable driving force for p-doping as the redox reaction with $FeCl_3$, considering just the standard redox potential of Fe^{3+}/Fe^{2+}equal to 0.771 V. We may note, however, that our Δf value is smaller by a factor of 10 than the value, estimated by Pichler et al. [13] for chemical doping with $FeCl_3$ (0.05 h^+/C-atom; 0.9 eV Fermi level shift). The difference might be rationalized, if we assume higher temperature needed for $FeCl_3$ doping. In fact, $FeCl_3$ is known to disproportionate in vacuum at elevated temperature:

$$2\ FeCl_3 \leftrightarrow 2FeCl_2 + Cl_2 \quad (5)$$

which would provide the redox potential of Cl_2/Cl^- equal to 1.36 V. However, the temperature reported by Pichler et al. [13] for peapods doping was 300 K only. This is, presumably, a printing error in the source Ref. [13], as the $FeCl_3$ doping requires vaporization of $FeCl_3$ at temperatures around 573 K [18,19]. Hence, small amount of Cl_2 can be present in the reaction mixture at this temperature, which would provide rational for stronger p-doping reported by Pichler et al. [13].

Obviously, the (electro)chemical doping of peapods is a complex process interfacing net charge transfer with the doping-specific chemistry of peapods. We have recently presented a first study combining electrochemical and K-vapor doping of peapods [14]. Comparison of both doping techniques allowed unexpected localization of potassium inside and outside the doped peapods [14]. This conclusion was recently confirmed by direct TEM observation [20]. The present paper upgrades this study by a first investigation of the reaction of peapods with potassium dissolved in mercury (K-amalgam) and by the comparison of amalgam- and vapor-doping techniques. In addition, data are presented for chemical p-doping with diluted F_2. A clear motivation for detailed studies of doping is the existence of many open questions, persisting notoriously even at the level of the parent SWCNT [21]. Concerted application of chemical and electrochemical doping is important to establish the common trends and to improve our understanding of the doping-induced effects in Raman spectra [21].

2. Experimental

The sample of C_{60}@SWCNT peapods (filling ratio 85%) [6] was available from our previous works [10,14,16]. A piece of peapod buckypaper was outgassed at 450 K/10^{-5} Pa (the residual gas was He). Potassium (from BDH) was purified by repeated distillation in vacuum. Subsequently, the potassium vapor was contacted at 450 K with the outgassed peapod buckypaper for 40 h. The reaction took place in an all-glass ampoule interconnected to a Raman optical cell, which was equipped with a Pyrex glass window. The rest of K was finally distilled off at 470 K/10^{-5} Pa into the cooled opposite end of the ampoule. Potassium amalgam was prepared under vacuum by dissolving potassium metal (BDH) in polarographic grade mercury and filtered twice through a glass capillary. The final concentration of K in the amalgam was 1.3 at%, as determined by acidimetric titration. All operations were carried out in sealed all-glass vacuum apparatus, which was interconnected to the Raman optical cell via magnetically breakable joint. The doping was realized by dipping of the peapod buckypaper into the amalgam. At room temperature, no significant changes of the Raman spectrum were traced, even after days of contact. Significant changes were observed only at higher temperatures of 100–150 °C. Chemical p-doping was carried out with F_2/Ar mixture (5/95% v/v) at room temperature for 2.5 h.

Spectroelectrochemical experiments employed a Pt-supported thin-film of peapods, which was fabricated by evaporation of the sonicated ethanolic slurry. The working electrode was outgassed overnight at 90 °C in vacuum (10^{-1} Pa) and then mounted in a spectroelectrochemical cell in a glove box under nitrogen. The cell was equipped with Pt-counter and Ag-wire pseudo-reference electrodes. The pseudo-reference potential was calibrated after adding small amount of ferrocene at the end of each spectroelectrochemical test. Hence, all potentials were referred to the ferrocene reference electrode, Fc/Fc^+. The electrolyte solution was either 0.2 M $LiClO_4$ in dry acetonitrile (Aldrich) or ionic liquid, viz, 1-butyl-3-methylimidazolium tetrafluoroborate (Fluka). The ionic liquid was purified and dried as described elsewhere [16]. The mass of peapod sample on top of Pt-support was assayed from the capacitive charge measured by cyclic voltammetry (Eq. (2)). (For a typical cyclic voltammogram of C_{60}@SWCNT in acetonitrile or in ionic liquid media see Ref. [9] or [16], respectively). The capacitance ($C \approx 40$ F/g) was determined for a peapod film of known mass, m; the film was weighed by quartz crystal microbalance as described elsewhere [22,23]. Electrochemical doping was carried out potentiostatically (PG 300 (HEKA) potentiostat). The working potential was −1.8 V (n-doping) or 1.1 V (p-doping). The Raman spectra were measured on a T-64000 spectrometer (Instruments, SA) interfaced to an Olympus BH2 microscope; the laser power impinging on the sample or cell window was between 1 and 5 mW. Spectra were excited by Ar^+ laser at 2.41 and 2.54 eV (Innova 305, Coherent). The Raman

spectrometer was calibrated before each set of measurements by using for reference the F_{1g} line of Si at 520.2 cm^{-1}.

3. Results and discussion

3.1. Raman spectra of n-doped C_{60}@SWCNT

Fig. 1 surveys the n-doping induced changes of the Raman spectra of C_{60}@SWCNT at the 2.41 eV excitation. (The spectra at 2.54 eV excitation (not shown) were qualitatively similar). The main effect, common to all of the used doping techniques, is a dramatic intensity quenching of the tube-related modes, i.e. the RBM and G-bands. The quenching arises from doping-induced changes of the population of electronic states near the Fermi level of peapods. Fig. 1 evidences that wider tubes (RBMs around 160 cm^{-1}) are more significantly doping-quenched compared to narrower tubes (RBMs around 175 cm^{-1}). This is due to smaller E_{33}^{S} separation for wide tubes, which translates into smaller driving force required for efficient doping of wider tubes [10,23]. The drop of Raman intensities at 2.41–2.54 eV excitation (cf. Fig. 1 and Ref. [10]) indicates blocking of the E_{33}^{S} transition, i.e. the Fermi level is shifted by more than 0.9 eV [13]. This seems to be plausible for K-vapor and K-amalgam doping. However, electrochemical charging at −1.8 V vs. Fc/Fc^{+} hardly provides more than ca. 0.01 e^{-}/C-atom (Eq. (4)), i.e. the Fermi level shift would not be sufficient in terms of the rigid band model [13]. Generally, the complex dependence of the Fermi level on applied potential [24], electrochemically-induced perturbations of the energy levels [25], variations in work functions of individual tubes and solvation of ions [26] should be taken into account for deeper discussion of the intensity/potential profiles. Table 1 surveys the frequencies of significant Raman lines, which demonstrate doping-induced changes. They comprise the A_g and H_g modes of intratubular C_{60} and the tangential displacement modes of the nanotube pod: G^{+} and G^{-} for displacement along the tube axis (LO phonon mode) and along the circumferential direction (TO phonon mode), respectively.

3.1.1. Fullerene C_{60}-related Raman lines: n-doping

When the pristine sample (Fig. 1, spectrum A) is treated with K-amalgam at 423 K for 40 h (spectrum C), the $A_g(2)$ peak softens by 29 cm^{-1} and looses its high-frequency satellite, $A_g(2)'$. This softening is equivalent to a transfer of 4–5 electrons per cage [14]. For the K-vapor doped sample (spectrum D) the $A_g(2)$ mode softens by 35 cm^{-1} and looses the satellite, too. The latter frequency shift is consistent with earlier works

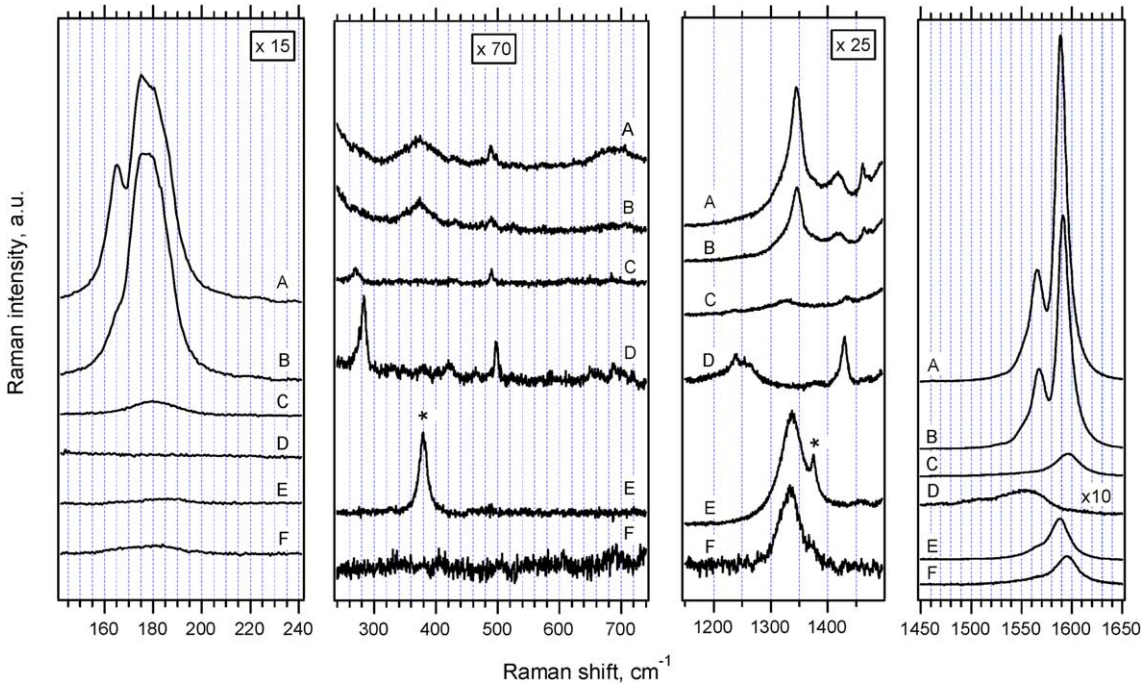

Fig. 1. Raman spectra of C_{60}@SWCNT (peapods) excited at 2.41 eV. [A] Pristine sample measured in air, [B] sample treated with K-amalgam at 423 K for 40 h, measured in air, [C] as sample B, but measured without contact to air in situ, [D] sample treated with K-vapor at 450 K for 40 h, measured in situ, [E] sample treated electrochemically at −1.8 V vs. Fc/Fc^{+} in 0.2 M $LiClO_4$ + acetonitrile, measured in situ. Acetonitrile bands are labeled by asterisk. [F] sample treated electrochemically at −1.8 V vs. Fc/Fc^{+} in 1-butyl-3-methylimidazolium tetrafluoroborate, measured in situ. Intensities were normalized by using the F_{1g} mode of silicon. Spectra are offset for clarity, but the intensity scale is identical for all spectra in the respective window, except the curve D (last right panel), which is zoomed by a factor of 10 in the intensity scale.

Table 1
Frequencies of the major Raman lines of C_{60}@SWCNT, exhibiting pronounced sensitivity towards doping (in cm^{-1}, excitation at 2.41 eV)

	$A_g(1)$	$A_g(2)$	$A_g(2)'$	$H_g(1)$	$H_g(2)$	G^+	G^-
Pristine sample	488	1463	1473	271	430	1590	1565
n-doped by K-amalgam, 40 h, 423 K	490	1434	–	270	429	1596	–
ditto exposed to air	489	1462	1473	269	430	1591	1568
n-doped by K-vapor, 40 h, 450 K	496	1428	–	284	423	1552	1510
ditto exposed to air	490	1440	–	276	429	1590	1565
n-doped electrochem. in acetonitrile sol.	–	1462	–	–	–	1588	1568
n-doped electrochem. in ionic liquid	–	–	–	–	–	1596	–
p-doped by 5 vol%, F_2, room temp.	488	1463	–	269	–	1594	1573
p-doped electrochem. in acetonitrile sol.	490	1464	–	275	432	1609	1586
p-doped electrochem. in ionic liquid	489	1465	–	275	432	1608	1585

No value (–) means that the band was not found in the spectrum. For details about the sample preparation and doping treatment, see Section 2. Electrochemical n-doping or p-doping was carried out at −1.8 V Fc/Fc^+ or 1.1 V vs. Fc/Fc^+, respectively.

[11,13,14] reporting on intratubular C_{60}^{6-} or $(C_{60}^{6-})_n$ [11,13]. We should also note the remarkably enhanced intensity of the Raman scattering from intratubular fulleride in the K-vapor doped sample (curve D). There is another striking difference between K-vapor and K-amalgam doping, if we inspect the doped materials after their exposure to ambient air. The K-vapor doped sample (curve D) is not fully recoverable to the state of neutral C_{60} in air and water, but part of the intratubular fullerene still survives in the C_{60}^{4-} state (cf. Ref. [14]). On the other hand, the K-amalgam doped sample (curve C) spontaneously recovers to the undoped state upon short (min) contact to ambient air. The characteristic $A_g(2)/A_g(2)'$ doublet of neutral peapod is thus restored, albeit with smaller intensity (spectrum B).

The hysteresis in re-oxidation of K-vapor doped peapods was previously interpreted as a result of partial localization of K^+ in the interior of peapod [14], where it can be even traced by TEM [20]. Also empty SWCNT can accommodate potassium inside the tubes [21]. The intratubular K^+ in peapods can promote the polymerization of C_{60} [11,13], since this reaction is driven by the counterion [27]. In any case, the intratubular fulleride of a formal composition of K_4C_{60} is air-stable [14]. On the other hand, the absence of polymerization and rapid re-oxidation of K-amalgam-doped peapods (curves B and C) points to the exclusive location of K^+ outside the n-doped peapod. Two arguments may elucidate the difference: (i) The standard redox potential of K^+/K is by ca. 1 V more negative than the corresponding redox potential of K-amalgam (−2.934 V against −1.975 V) [28]. (ii) Because of the high-surface tension, the amalgam cannot penetrate into nanosized pores of the peapods. This provides rational for sluggish amalgam doping at room temperature (see Section 2), as the K^+ ions must, eventually, be located inside the voids between the n-doped peapods in a bundle. The layer of K^+ ions at the outer surface of peapod, must compensate not only the charge at SWCNT pod, but also at the intratubular fulleride anions, C_{60}^{4-} or C_{60}^{5-}. The electron transfer between SWCNT and C_{60} should be fast and efficient enough at these conditions [10,29].

The radial breathing $A_g(1)$ mode hardens by 2 cm^{-1}in K-amalgam doped peapods and 8 cm^{-1} in K-vapor doped peapods (Table 1 and Fig. 1A, C and D). Analogous blue shift is apparent also for the $H_g(1)$ mode. This line exhibits marked intensity increase, both in K-amalgam and especially in the K-vapor doped samples (Fig. 1C and D). These results are in qualitative accord with the data reported by Pichler et al. [11,13]. The remarkable enhancement of the $H_g(1)$ mode is unique, and is not reproduced for the remaining $H_g(2)$ to $H_g(7)$ modes (the $H_g(8)$ mode cannot be analyzed as it is overlapped by the G-band).

Electrochemical reduction at −1.8 V vs. Fc/Fc^+ provides still less efficient charge transfer than the amalgam doping. In contrast to chemical doping with potassium, all the Raman bands of intratubular C_{60} are attenuated and are hardly detectable. In some spectra, we can only trace a weak band of $A_g(2)$, which shows no frequency shift compared to that in pristine peapod. Hence, the electrolyte cations compensate the negative charge on SWCNT wall, which is not coupled to pronounced charging of intratubular C_{60}. However, interpretation of the strong quenching of intensities upon cathodic n-doping is still unclear.

3.1.2. G-band: n-doping

The frequency and intensity of SWCNT-related G-band are sensitive to doping, but there is a serious controversy in the literature how to interpret the experimental data [21]. The confusion comes from the fact that, depending on the doping method, SWCNT may or may not show monotonous changes of G-band frequency upon progressive n-doping [23,30–34]. The observed frequency shifts do not seem to be elucidated in terms of any available theory of SWCNT nor graphene at the moment [21]. The simplest model would predict that extra electrons in the π-band of n-doped graphene cause expansion of graphene (C–C bonds) and thus

downshift of the G-band frequency. For p-doping of graphene, a mirror effect is expected, i.e. C–C contraction and G-frequency upshift, albeit this trend may not be theoretically monotonous, too [21,35].

Our data in Fig. 1 and Table 1 are phenomenologically consistent with the concept of non-monotonous G-band shifts. Of particular interest is the blue-shifted, single Lorentzian G-band upon K-amalgam doping (Fig. 1, curve C). This situation is reminiscent of the final stage of Interval III doping of SWCNT with Cs-vapor [21]. The K-amalgam allows selective charge transfer towards a material exhibiting solely this anomalous n-doping response. Our spectrum (Fig. 1, curve C) was traced for the end-product of amalgam doping, which does not change after days of contact of both reactants at 150 °C. This is an explicit advantage of amalgam doping over vapor doping, since the Interval III is rather short in time during continuous vapor doping [21].

Upon K-vapor doping, we can trace strongly red-shifted G-band with Fano-broadening (Fig. 1, curve D) which reflects the high-electron concentration in the π-band. We detect a distinct new band at 1250 cm^{-1}, which is a characteristic signature of heavy doping [21,30], albeit of still unclear origin [21]. Obviously, our data match those of Chen et al. [21] for Cs/SWCNT system. On the other hand, our data are in conflict with those of Pichler et al. [13] for K/peapod system, reporting upshift of the G-line to 1605 cm^{-1}. The discrepancy can be rationalized, assuming that the Pichler et al.'s data do not address the final stage of K-vapor doping, i.e. the used maximum reaction time (24 h) [13] does not seem to be sufficient for complete vapor doping. This is also supported by the fact that our RBM intensity drops to zero after 40 h of reaction (Fig. 1, curve D; cf. also Ref. [21]), whereas the RBM is still clearly traced after 24-h K-doping [13].

Cathodic doping in acetonitrile electrolyte solution (Fig. 1, curve E) causes the "normal" monotonous downshift of G-band, without any intermediate hardening between the open circuit potential to ca. −1.8 V (cf. also Ref. [9,10]). This matches the behavior of empty SWCNT in the same electrolyte solution [23]. However, more detailed analysis shows that this behavior is not generally valid for all electrochemical media. Explicitly in ionic liquids (Fig. 1, curve F), we observe just the opposite effect: the upshift of G-mode by 6 cm^{-1} at −1.8 V and single Lorentzian shape similar to that after K-amalgam doping. If we sweep the potential from open circuit to about −2.4 V, the G-band hardens monotonously by ca. 10–15 cm^{-1}, both in C_{60} peapods and empty SWCNT [16]. Eventually, non-monotonous shifts in SWCNTs were also traced for certain other electrolyte solutions [21]. The doping-induced response in ionic liquid is similar to that upon K-amalgam doping or early stages of K- or Cs-vapor doping [13,21]. This would point to the conclusion that the absence of solvent in ionic liquid mimics the conditions of chemical doping.

3.2. Raman spectra of p-doped C_{60}@SWCNT

Fig. 2 surveys the p-doping driven changes of the Raman spectra of C_{60}@SWCNT at the 2.54 eV excitation. (The spectra at 2.41 eV excitation (not shown) were qualitatively similar). As expected [10–13], the blue laser (2.54 eV) gives the optimum resonance with the C_{60} optical transitions in pristine peapods (cf. curves A in Figs. 1 and 2). Analogously, we trace dramatic attenuation of RBM and G-mode intensities as for n-doping (Section 3.1). As in the case of n-doping (Section 3.1) we may note the preferential quenching of RBM of wider tubes (at ca. 160 cm^{-1}) for all doping techniques used (cf. Figs. 1 and 2).

The most striking effect in electrochemically p-doped peapods is the massive growth of Raman intensities of intratubular C_{60}, (curves C, D and Refs. [10,14,16]). This peculiar effect, called "anodic Raman enhancement" is unique for electrochemical oxidation of C_{60} peapods, both in acetonitrile electrolyte solutions and in ionic liquids [16], but it is absent in C_{70} peapods [10]. We have previously suggested an interpretation based on hybridization of the π-orbitals of C_{60} with nearly free-electrons of SWCNT [10]; the key arguments followed from the mutual positions of t_{1u} orbital of C_{60} against the Fermi level of SWCNT [10,29]. This hypothesis inherently assumes that the anodic enhancement is solely of electronic origin, i.e. the changes in population of states near the Fermi level are responsible for the corresponding changes in Raman intensities. This dependence should be invariant of the method of doping (dopant). Contrary to this interpretation the chemical p-doping of peapods, promoted by $FeCl_3$, did not reproduce any "anodic enhancement" [13]. Actually, Pichler et al. [13] reported on similar or even smaller intensities of $A_g(2)$ and $H_g(7)$ upon progressive interaction of peapods with $FeCl_3$ vapor.

To investigate this peculiarity further, we have chosen a very strong oxidant (F_2). Preliminary experiments showed that pure F_2 reacts rapidly with peapods, causing their chemical fluorination, and a complete disappearance of the tube-specific Raman modes (e.g. RBM). On the other hand, fluorine diluted with inert gas (Ar, N_2) to concentration of ca. 5–20 vol% does not cause complete destruction of the sample, while we may trace also the peapod-specific Raman scattering.

Curve B in Fig. 2 confirms that there is no "anodic enhancement", but monotonous drop of all Raman bands of peas and pods upon progressive fluorination (except the D-band, which grew as a result of increased disorder). We assume that the so far used oxidants, F_2, $FeCl_3$ (or Cl_2, see Eq. (5)) actually do not act as

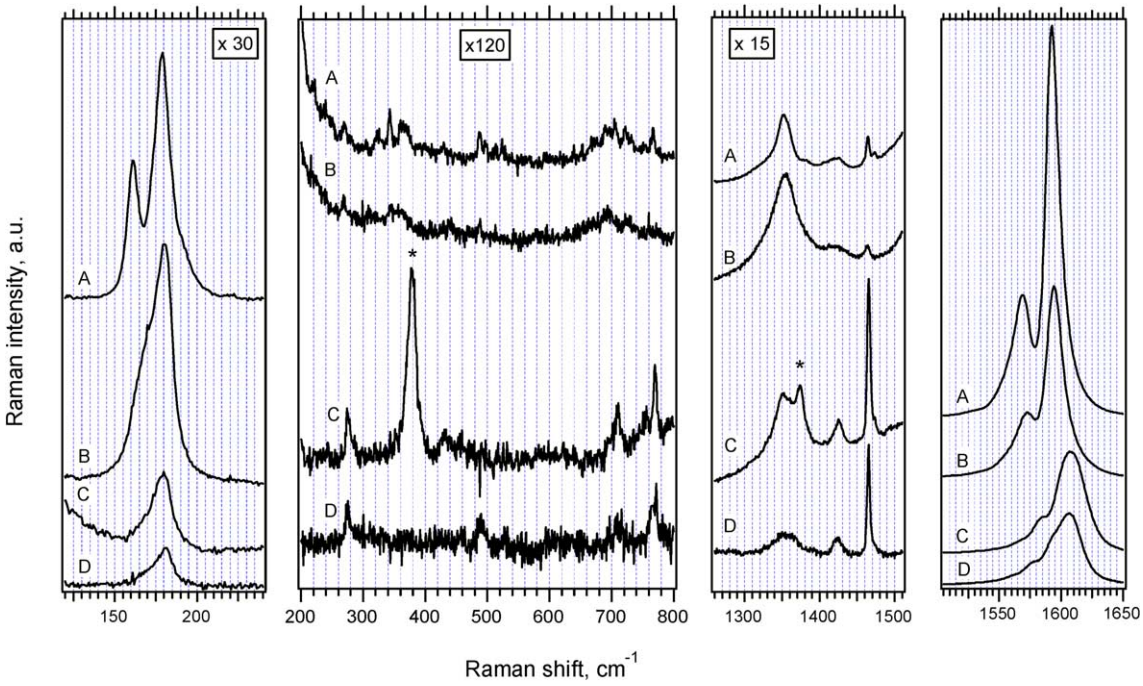

Fig. 2. Raman spectra of C_{60}@SWCNT (peapods) excited at 2.54 eV. [A] pristine sample measured in air, [B] sample treated with 5% F_2/Ar (v/v) at room temperature for 2.5 h, [C] sample treated electrochemically at 1.1 V vs. Fc/Fc^+ in 0.2 M $LiClO_4$ + acetonitrile, measured in situ. Acetonitrile bands are labeled by asterisk. [D] sample treated electrochemically at 1.1 V vs. Fc/Fc^+ in 1-butyl-3-methylimidazolium tetrafluoroborate, measured in situ. Spectra are offset for clarity, but the intensity scale is identical for all spectra in the respective window. Intensities were normalized by using the F_{1g} mode of silicon.

net h^+ donors (Eq. (1a)), but they may cause irreversible chemical changes of the peapods. (The n-doping with potassium metal is, presumably, less disturbed by chemical reactions, cf. Section 3.1 and Eq. (1b)). Obviously, electrochemistry is the ideal technique for clean p-/n-doping, since parasitic chemical side reactions are minimized or excluded in the electrochemical environment.

The p-doping induced changes of G-band are less complicated than the changes after n-doping (Section 3.1.2.). We always observe intensity attenuation along with monotonous frequency upshift (Fig. 2). The same behavior is traced for anodic p-doping of peapods and empty SWCNT both in classical electrolyte solutions [10,23] and in ionic liquids [16]. This behavior also matches the expected contraction of graphene C–C bond induced by p-doping [21].

4. Conclusions

Parallel application of chemical and electrochemical doping reveals various peculiarities in the Raman spectra of p-/n-doped C_{60}@SWCNT. The data collected in this work, along with those reported previously in the literature, evidence a complex nature of doping. This is highlighted by explicit dependence of the Raman response, both of the pea and pod subunits, on the chosen doping technique and on the sample environment in electrochemical experiments. These effects demonstrate that the simple model of tuning of electronic states of peapods can hardly explain the complicated feedback of C_{60}@SWCNT to redox doping.

Reaction of peapods with potassium amalgam produces a material, exhibiting the anomalous n-doping response with blue-shifted G-band and the charging state of intratubular C_{60} being 4–5 electrons per cage. This doping is fully recoverable upon short contact of the samples to ambient air. The charge-compensation by unsolvated K^+ counterions, which are located solely at the outer surface of peapod is similar to the case of electric double layer in ionic liquid. On the other hand, gaseous potassium causes deep reduction of peas to C_{60}^{6-} and the K^+ counterions also penetrate into the interior of peapod. A complete reaction with K-vapor requires equilibration time exceeding 24 h.

A significant enhancement of Raman scattering of intratubular fullerene is traced in electrochemically p-doped peapods, independently of the electrochemical medium used. However, this peculiar anodic Raman enhancement is not reproduced for chemically p-doped peapods with diluted F_2. We suggest that the absence of an enhancement is due to irreversible chemical modification of peapods. The p-doping of peapods causes monotonous G-band upshift for all the p-doping techniques employed, and resembles the p-doping of

graphene. This simple picture contrasts with a complicated behavior of G-band in n-doped peapods.

Acknowledgements

This work was supported by IFW Dresden, Academy of Sciences of the Czech Republic (Contract No. A4040306) and by Czech Ministry of Education Youth and Sports (Contract No. LC-510). We are grateful to Dr. Jiri Uhlir, Institute of Nuclear Research, Rez, CZ for treatment of samples in F_2.

References

[1] Smith BW, Monthioux M, Luzzi DE. Encapsulated C_{60} in carbon nanotubes. Nature 1998;396:323–4.
[2] Burteaux B, Claye A, Smith BW, Monthioux M, Luzzi DE, Fischer JE. Abundance of encapsulaetd C_{60} in peapods. Chem Phys Lett 1999;310:21–4.
[3] Bandow S, Takizawa M, Hirahara K, Yudasaka M, Iijima S. Raman scattering study of double-wall carbon nanotubes. Chem Phys Lett 2001;337:48–54.
[4] Hirahara K, Suenaga K, Bandow S, Kato H, Okazaki T, Shinohara H, et al. Metallofullerne peapods. Phys Rev Lett 2000;85:5384–7.
[5] Kataura H, Maniwa Y, Kodama T, Kikuchi K, Hirahara K, Suenaga K, et al. High yield fullerene encapsulation in single-wall carbon nanotubes. Synth Met 2001;121:1195–6.
[6] Kataura H, Maniwa Y, Abe M, Fujiwara A, Kodama T, Kikuchi K, et al. Optical poperties of fullerene and non-fullerene peapods. Appl Phys A 2002;74:349–54.
[7] Kuzmany H, Pfeifer M, Kramberger C, Pichler T, Liu X, Knupfer M, et al. Analysis of the concentration of C_{60} fullerenes in single-wall carbon nanotubes. Appl Phys A 2002;76:449–56.
[8] Liu X, Pichler T, Knupfer M, Golden MS, Fink J, Kataura H, et al. Filling factors, structural and electronic properties of C_{60} in single-wall carbon nanotubes. Phys Rev B 2002;65:045419–0454196.
[9] Kavan L, Dunsch L, Kataura H. In situ Vis–NIR and Raman spectroelectrochemistry at fullerene peapods. Chem Phys Lett 2002;361:79–85.
[10] Kavan L, Dunsch L, Kataura H, Oshiyama A, Otani M, Okada S. Electrochemical tuning of electronic structure of C_{60} and C_{70} fullerene peapods: in-situ Vis–NIR and Raman Study. J Phys Chem B 2003;107:7666–75.
[11] Pichler T, Kuzmany H, Kataura H, Achiba Y. Metallic polymers of C_{60} inside single-wall carbon nanotubes. Phys Rev Lett 2001; 87:267401–14.
[12] Pfeiffer R, Kuzmany H, Pichler T, Kataura H, Achiba Y, Melle-Franco M, et al. Electronic and mechanical coupling between guest and host in carbon peapods. Phys Rev B 2004;69: 0354041–47.
[13] Pichler T, Kukovecz A, Kuzmany H, Kataura H, Achiba Y. Quasicontinuous electron and hole doping of C_{60} peapods. Phys Rev B 2003;67:125416–1254167.
[14] Kalbac M, Kavan L, Zukalova M, Dunsch L. Two positions of potassium in chemically doped C_{60} peapods: an in situ spectroelectrochemical study. J Phys Chem B 2004;108:6275–80.
[15] Liu X, Pichler T, Knupfer M, Fink J, Kataura H. Electronic properties of K-intercalated peapods. Phys Rev B 2004;69: 0754171–77.
[16] Kavan L, Dunsch L. Ionic liquids for in-situ Vis–NIR and Raman spectroelectrochemistry: doping of carbon nanostructures. Chemphys chem 2003;4:944–50.
[17] Kavan L, Dunsch L. Diameter selective electrochemical doping of HiPco single wall carbon nanotubes. Nano Lett 2003;3:969–72.
[18] Kukovecz A, Pichler T, Pfeiffer R, Kuzmany H. Diameter selective charge transfer in p- and n-doped single-wall carbon nanotubes. Chem Commun 2002:1730–1.
[19] Kukovecz A, Pichler T, Kramberger C, Kuzmany H. Diameter selective doping of single-wall carbon nanotubes. Phys Chem Chem Phys 2003;5:582–7.
[20] Guan L, Suenaga K, Shi Z, Gu Z, Iijima S. Direct imaging of alkali metal site in K-doped fullerene peapods. Phys Rev Lett 2005;94:045502–0455024.
[21] Chen G, Furtado CA, Bandow S, Iijima S, Eklund PC. Anomalous contraction of the C–C bond length in semiconducting carbon nanotubes observed during Cs doping. Phys Rev B 2005;71:045408–0454086.
[22] Kavan L, Rapta P, Dunsch L. In situ Raman and Vis NIR spectroelectrochemistry at single-walled carbon nanotubes. Chem Phys Lett 2000;328:363–8.
[23] Kavan L, Rapta P, Dunsch L, Bronikowski MJ, Willis P, Smalley RE. Electrochemical tuning of electronic properties of single walled carbon nanotubes: in-situ Raman and Vis–NIR study. J Phys Chem B 2001;105:10764–71.
[24] Rubim JC, Corio P, Riberiro MCC, Matz M. Surface enhanced Raman on electrode surface. J Phys Chem 1995;99:15765–74.
[25] Corio P, Santos PS, Brar VW, Samsonidze GG, Chou SG, Dresselhaus MS. Potential dependent surface Raman spectroscopy of carbon nanotubes. Chem Phys Lett 2003;370:675–82.
[26] Okazaki K, Nakato Y, Murakoshi K. Absolute potential of the Fermi level of isolated SWCNT. Phys Rev B 2003;68: 035434–0354345.
[27] Lu J, Nagase S, Zhang S, Peng L. Counterion driven polymerization of C_{60}. Chem Phys Lett 2004;395:199–204.
[28] Korshunov VN. Electrochemical properties of alkali and alkaline earth metals amalgam. Itogi Nauki Tekh Ser Elektrokhim 1988;26:94–193.
[29] Dubay O, Kresse G. Density functional calculation for peapods. Phys Rev B 2004;70:165424–10.
[30] Rao AM, Eklund PC, Bandow S, Thess A, Smalley RE. Evidence for charge transfer in carbon nanotube bundles from Raman scattering. Nature 1997;388:257–9.
[31] Claye A, Rahman S, Fischer JE, Sirenko A, Sumanasekera GU, Eklund PC. In-situ Raman scattering in alkali-doped single-wall carbon nanotubes. Chem Phys Lett 2001;333:16–22.
[32] Bendiab N, Anglaret E, Bantignies JL, Zahab A, Sauvajol JL, Petit P, et al. Stoichiometry dependence of the Raman spectrum of alkali doped single-wall carbon nanotubes. Phys Rev B 2001;64:245424–2454246.
[33] Bendiab N, Spina L, Zahab A, Poncharal P, Marliere C, Bantignies JL, et al. Combined in-situ conductivity and Raman studies of Rb doping of single-wall carbon nanotubes. Phys Rev B 2001;63:153407–1534074.
[34] Claye A, Nemes NM, Janossy A, Fischer JE. Structure and electronic properties of K doped single-wall carbon nanotubes. Phys Rev B 2000;62:R4845–8.
[35] Verissimo-Alves M, Koiller B, Chacham H, Capaz RB. Electromechanical effects in carbon nanotubes: ab initio and analytical tight binding calculations. Phys Rev B 2003;67:161401–4.